論 文

Y-branch Directional Coupler Optical Switch/Modulator

Chang Min Kim*, Sang Pil Han*, Nag Un Song** *Regular Members*

Y-분기 방향성 결합기 광 스위치/변조기

正會員 金 昌 敏* 正會員 韓 相 弼* 正會員 宋 洛 雲**

ABSTRACT

Y-branch directional coupler optical switches with two different coupling lengths are fabricated on z-cut LiNbO$_3$ and tested at $\lambda = 1.3 \, \mu$m. The normal mode and coupled mode theories are utilized to calculate devices' coupling length and switching voltage. Simulation of the beam propagation method (BPM) is also performed to confirm the devices' coupling lengths. For dc operation, experimental results are in good agreement with the modee theories' expectation.

要 約

두개의 다른 결합길이를 갖는 Y-분기 방향성 결합기 광스위치를 z-cut LiNbO$_3$로 제작하였고, $\lambda = 1.3 \mu$ m에서 테스트하였다. 소자의 결합길이를 계산하기 위하여 정상모드 이론과 결합모드 이론을 사용하였다. 빔전송 이론의 전산모의를 통하여 소자의 결합길이를 재 확인하였다. 직류동작시 실험 결과치들이 결합모드 이론에 의한 예측치와 잘 부합 하였다.

I. Introduction

High-speed optical modulators are important components in wide-band single-mode optical communication systems. Such systems are very attractive as they provide high capacity data links due to their small group velocity dispersion and low loss at 1.3μm. Electrooptic external modulators using LiNbO$_3$ waveguides are potentially use-ful devices for high bit rate transmissions and signal processing.

Several types of external optical modulators have been proposed up-to-date : cut-off type, uniform directional coupler (DC), alternating $\Delta\beta$ DC, Mach-Zehnder, crossed coupler and Y-branch DC.

There are a number of design parameters that determine the ultimate performance of Ti-indiffused LiNbO$_3$ modulators : a good frequency response, a low switching voltage and high extinction ratio. As these factors are not independent but related with each other, an appropriate trade-

* 서울市立大學校 電子工學科
  Dept. of Electronics Engineering Seoul City University.
** 弘益大學校 電子工學科
  Dept. of Electronics Engineering, Hong-ik University
論文番號 : 93－114

off is required depending on the factor we emphasize.

Among them, the uniform DC optical modulator has been widely used and preferred since most intensity modulators are based on the theory of the uniform DC. Recently, Y-branch DC optical modulator has been proposed [1] and known to have a definite advantage over the uniform DC. The coupling length of the Y-branch DC is shorter than that of the uniform DC by the factor of $1/\sqrt{2}$ while preserving the lower switching voltage and the same extinction ratio. This is one of the important factors in achieving the high-speed switching and modulation.

In this work, the coupled mode theory is introduced to analyze Y-branch DC optical switches. By use of the theory, the device's switching voltage can be approximately formulated. Secondly, the normal mode analysis is applied to find exact coupling length by use of a combination of the effective index method (EIM) and the 1-dimensional finite difference method (1-D FDM). Thirdly, the BPM [2] is used to confirm that calculation results obtained by the mode theories are appropriate.

The BPM relates the field distribution at a certain plane of z with that at the next plane of z, based upon the difference of refractive index profiles of two planes. The method is capable of figuring out the variation of beam shape along the z-axis of beam propagation.

In the expriment, two devices with different coupling lengths are fabricated on z-cut LiNbO₃ substrate and tested at $\lambda = 1.3$ ㎛. The experimental results are compared with the mode theories' expectation.

II. Theory and Design

A. Coupled Mode Analysis

The schematic diagram of a Y-branch DC optical switch is depicted in the Fig.1. Optical waveguides structure including the branching section and the parallel directional coupler section are symmetric. The shaded region represents the ele-
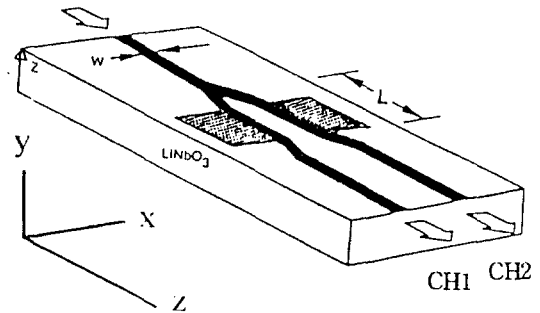

Fig. 1. Y-branch DC optical switch (shaded region: electrodes) Substrate: z-cut LiNbO₃ (Y-plane), $\lambda = 1.3$ ㎛

ctrode section, through which the electric field is applied to induce the electrooptic effect.

We denote the exact coupling lengths (for the first complete power transfer) of the uniform DC and Y-branch DC by l_c and l_y, respectively. The actually fabricated device's coupling length (parallel arms' length) is expressed as L.

The coupled mode theory analyzes each waveguide of parallel arms seperately and evaluates the degree of coupling based on the perturbation theory. Coupled mode equation of an uniform DC is, in general, represented as [3]

$$\begin{bmatrix} R \\ S \end{bmatrix} = \begin{bmatrix} \cos(\frac{\pi}{2}r) + j\frac{x}{r}\sin(\frac{\pi}{2}r) & -j\frac{y}{r}\sin(\frac{\pi}{2}r) \\ -j\frac{y}{r}\sin(\frac{\pi}{2}r) & \cos(\frac{\pi}{2}r) - j\frac{x}{r}\sin(\frac{\pi}{2}r) \end{bmatrix}$$

$$\begin{bmatrix} R_o \\ S_o \end{bmatrix} \tag{1}$$

where $x = \Delta\beta L/\pi$, $y = L/l_c$, $\Delta\beta = |\beta_1 - \beta_2|$ and

$$r^2 = x^2 + y^2 \tag{2}$$

β_1 and β_2 represent the propagation constants of each arm waveguide. $\Delta\beta$ could be the electrooptically induced propagation constants' difference between two waveguides due to the applied voltage. Without any applied voltage, $\Delta\beta$ will be zero since two parallel arms are symmetric in this work.

The light of $\lambda = 1.3$ ㎛ is launched into an op-

1109

tical waveguide input and, then, the launched power is evenly divided due to the symmetry of the branching section. As the power is divided by halves at beginning of the DC section, we put $R_o = S_o = 1/\sqrt{2}$ so that $S_o S_o^* = R_o R_o^* = 1/2$. Eq.(1), then, reduces to

$$R R^* = \frac{1}{2} \left[1 - \frac{2xy}{r^2} \sin^2(\frac{\pi}{2} r) \right] \qquad (3a)$$

$$S S^* = \frac{1}{2} \left[1 + \frac{2xy}{r^2} \sin^2(\frac{\pi}{2} r) \right] \qquad (3b)$$

Complete power transfer occurs

$$R R^* = o, \qquad \text{when } x = y = 1/\sqrt{2} \qquad (4)$$

We now put L as l_y temporarily since l_y is the Y-branch DC's coupling length for the complete power transfer. The conditions of Eq.(4) can be rewritten as such

$$\Delta\beta = |\beta_1 - \beta_2| = \pi/(\sqrt{2} \ l_y) = \pi/l_c \qquad (5)$$

$$l_y = l_c/\sqrt{2} \qquad (6)$$

Eq.(5) means that $\Delta\beta$ needs to be created up to the value of $\pi/(\sqrt{2} \ l_y)$ so as to perform the switching operation. Eq.(6) implies that the coupling length of the Y-branch DC is shorter than that of the uniform DC by the factor of $1/\sqrt{2}$ if both DCs' structures are exactly the same. This is one of the important factors in achieving the high-speed modulation.

As $\Delta\beta$ is induced by an applied electric field E, $\Delta\beta$ could be possibly expressed in terms of applied switching voltage V_{sw}. To derive this, we begin with the index increment due to the V_{sw}.

$$n_{s1} = n_s \pm \delta n, \qquad n_{s2} = n_s \pm \delta n \qquad (7)$$

$$\delta n = (1/2 \ n_s^3 r_{33}) \cdot (\Gamma \frac{V_{sw}}{s}) \qquad (8)$$

n_s is the substrate index of LiNbO₃. n_{s1} and n_{s2} are the changed substrate index of each wave-

guide region in the presence of electric field. δn is the refractive index's increment due to the applied electric field. The index distribution change due to the applied electric field will be described in detail later. The electric field is induced in such a way that the refrative index of the beam-launched arm is increased. r_{33} is the electrooptic coefficient of z-cut LiNbO₃ substrate, and Γ is the overlap integral factor between the optical beam and the modulating electric field. s is the gap between the electrodes. $\Delta\beta$ is expressed in terms of mode index N.

$$\Delta\beta = |\beta_1 - \beta_2| = |N_1 - N_2| k_0 \qquad (9)$$

where k_0 is wavenumber in the vacuum. For weakly guiding cases, $|N_1 - N_2| k_0$ approximates

$$|N_1 - N_2| k_0 \approx |n_{s1} - n_{s2}| k_0 = 2 \ \delta n \ k_0 \qquad (10)$$

Most of LiNbO₃ devices belong to the weakly guiding case. Manipulating Eqs.(5) to (10), we have, for Y-branch DC,

$$V_{sw} = \frac{s \cdot \lambda}{2 \ n_s^3 r_{33} \ \Gamma \ (\sqrt{2} \ l_y)} \qquad (11)$$

Note from Eq.(11) that V_{sw} is inversely proportional to the coupling length l_y. For LiNbO₃, $n_s^3 r_{33} = 3.06 \times 10^{-1} \ \mu m/V$. We take Γ as 0.3 approximately throughout this work[4]. In order to design Y-branch DC optical switch devices, we need to find l_c or l_y first. By use of Eq.(11), we can approximately estimate the required switching voltage. In what follows, the normal mode analysis is used to calculate l_c with aid of the EIM and the 1-D FDM.

B. Normal Mode Analysis
I. Design parameters

The waveguides are fabricated on z-cut LiNbO₃ substrate. Ti strip dimensions of the Y-branch DC prior to the diffusion are as follows : 700 Å thick, 5 μm wide in all waveguides. 5 μm gap between parallel arms. The diffusant Ti is diffused at 1025

1110

℃ for 6 hours. With reference to [5], the diffusion length d_x and d_y are 3.2 μm and 3.2 μm, respectively.

It is assumed that the refractive index profile of a waveguide has Gaussian distribution along the depth direction while having a composite function of complementary Error function along the lateral direction [5]. The parallel arms' index profile of Fig.1 is now represented as

$$n(x,y) = n_s + \Delta n \cdot \exp\left[-(\frac{y}{d_y})^2\right] \cdot G(x) \qquad (12)$$

where n_s is the substrate refractive index and Δn is the top surface index increment of the channel due to the diffusion of Ti. Δn is the function of Ti width and thickness prior to the diffusion, and of diffusion time and temperature. Data of Δn are taken from [5].

$G(x)$, the horizontal refractive index profile along x-axis, is given by

$$G(x) = F(x - c_1, w) + F(x - c_2, w) \qquad (13)$$

where

$$F(x,w) = 1/2 \left[\operatorname{erf}(\frac{x+w/2}{d_x}) - \operatorname{erf}(\frac{x-w/2}{d_x})\right]$$
$$/ \operatorname{erf}(\frac{w/2}{d_x}) \qquad (14)$$

In the equations above, c_1 and c_2 are the center positions of each channel, and w is the Ti width of each channel prior to the diffusion.

2. Analysis

Since the waveguides are 2-dimensional (2-D), we convert the 2-D index profile to 1-D index profile (in terms of x-axis) by use of the EIM in order to reduce the abundant computation time. We first slice the guiding structure along the y-axis very thinly. We then calculate the fundamental mode index using the 1-D FDM and replace the slice with the earned mode index $N(x)$.

To follow up the above concept mathematically, we use the same technique used in [6]. The 2-

D Helmholtz equation may be seperated into two 1-D normalized equations.

$$[V_y^2 G(\xi)]^{-1} \frac{d^2}{d\eta^2} E_1(y) + [\exp(-\eta^2) - b(x)] \cdot E_1(y) = 0 \qquad (15)$$

$$V_x^{-2} \frac{d^2}{d\xi^2} E_2(x) + [G(\xi) b(x) - b] \cdot E_2(x) = 0 \qquad (16)$$

where $\xi = x/d_x$, $\eta = y/d_y$, $V_{x,y} = k \cdot d_{x,y} \sqrt{n_t^2 - n_s^2}$ $\qquad (17)$

$$b(x) = \frac{N^2(x) - n_s^2}{(n_t^2 - n_s^2) G(\xi)} \quad , \qquad n_t = n_s + \Delta n \qquad (18)$$

and $b = \dfrac{N^2 - n_s^2}{n_t^2 - n_s^2}$, $\qquad \beta = k_0 N \qquad (19)$

In Eq.(19), N and b are the final mode index and the normalized mode index of a given waveguide, respectively.

As seen from Eq.(15), $b(x)$ will be the function of $V_y G(\xi)^{1/2}$. The discrete set of $[b(x), V_y G(\xi)^{1/2}]$ can be easily obtained by the 1-D FDM technique. $b(x)$ is now approximated as a polynomial of $V_y G(\xi)^{1/2}$ by use of the least square method. We can then have the effective index distribution $N(x)$ by way of $b(x)$. The 2-D guiding structure of Fig. 1 is now replaced with 1-D effective index distribution $N(x)$ as in Eq.(18). The final mode index N and the corresponding field profile are to be calculated in Eq.(16) using the 1-D FDM with parameters of Eqs(17), (18) and (19).

In the normal mode theory, we consider two proximate parallel waveguides as a single waveguide structure and obtain a pair of even and odd fundamental modes. The beating mechanism of two modes explains the coupling phenomenon.

It is noted that l_c is the length of complete power transfer when no electric field is applied. With fabrication parameters given earlier, the calculated values of the even and odd fundamental modes β_e, β_o are

$$\beta_e = 10.40100 \ \mu\text{m}^{-1} \quad \text{and} \quad \beta_o = 10.40001 \ \mu\text{m}^{-1}$$

It is easily understood that the value of l_c is re-

1111

lated with the difference of β_e and β_o as such

$$l_c = \frac{\pi}{\beta_e - \beta_o} = 3.093 \text{ mm} \tag{20}$$

Using the above equation, we obtain

$$l_y = 2.187 \text{ mm} \quad \text{and} \quad V_{sw} = 11.45 \text{ V}$$

In the next section, we will check if the results we obtained above is acceptable with the aid of the BPM.

III. Beam Propagation Method (BPM)

A. Theory

The wave behavior of optical beam in the waveguides can be described by the Helmholtz equation

$$\nabla_t^2 E + \frac{\partial^2}{\partial z^2} E + k_0^2 n^2(x,y,z) E = 0 \tag{21}$$

where $\quad \nabla_t^2 = \frac{\partial^2}{\partial x^2} + \frac{\partial^2}{\partial y^2}$, $\qquad k_0 = \frac{\omega}{c}$

Putting

$$E(x,y,z) = \mathcal{E}(x,y,z) e^{-jk_s z}, \qquad k_s = \frac{\omega}{c} n_s \tag{22}$$

Eq. (21) is transformed to

$$j2k_s \frac{\partial \mathcal{E}}{\partial z} = [\nabla_t^2 + (k^2 - k_s^2)] \mathcal{E} \tag{23}$$

where $k = \frac{\omega}{c} n(x,y,z)$. k_0, k_s and k are the wave numbers in the air, substrate and waveguide, respectively. Note that in derivation of Eq. (23), $\partial^2 \mathcal{E} / \partial z^2$ is neglected.

We confine our interest to 2-D space of (x,z). Eq. (23), the paraxial wave equation, is rewritten to the equivalent form

$$\mathcal{E}(x,z) = \exp \left[\int_0^z \frac{1}{j2k_s} [\nabla_t^2 + (k^2 - k_s^2)] dz \right] \tag{24}$$

The relation between $\mathcal{E}(x, z+\Delta z)$ and $\mathcal{E}(x, z)$ is, therefore,

$$\mathcal{E}(x, z+\Delta z) = \exp \left[\int_z^{z+\Delta z} \left[\frac{\nabla_t^2}{j2k_s} + \frac{1}{j2k_s} (k^2 - k_s^2) \right] dz \right] \cdot \mathcal{E}(x, z) \tag{25}$$

Δz is a step size in the propagation direction. Eq. (25), with the error of $O(\Delta z^3)$, is approximated to

$$\mathcal{E}(x, z+\Delta z) = \exp \left[\frac{\Delta z}{j2k_s} \nabla_t^2 \right] \cdot \exp \left[\frac{k_s \Delta z}{j2} \left(\frac{n^2(x, z+\Delta z/2)}{n_s^2} - 1 \right) \right] \cdot \mathcal{E}(x, z) \tag{26}$$

Let's think about the propagation in a homogeneous medium for a moment. In a simple homogeneous medium such as a free space, Eq. (26) reduces to

$$\mathcal{E}(x, z+\Delta z) = \exp \left(\frac{\Delta z}{j2k_s} \nabla_t^2 \right) \cdot \mathcal{E}(x, z) \tag{27}$$

In treating the operator ∇_t^2 of Eq. (27), the Fourier transform is one of possible approaches to the solution.

$$\mathcal{E}_m(z) = \sum_{p=-N/2+1}^{N/2} \mathcal{E}(x_p, z) \cdot \exp(-j \frac{2\pi}{N} p \cdot m) \tag{28a}$$

$$\mathcal{E}(x_p, z) = \frac{1}{N} \sum_{m=-N/2+1}^{N/2} \mathcal{E}_m(z) \cdot \exp(j \frac{2\pi}{L} m \cdot x_p) \tag{28b}$$

Eqs. (28) represent the Fourier transform and inverse Fourier transform, respectively. In the equations, N is the number of sampling points and x_p is a sampled x position. L is the length of the computational grid. Eq. (27) is transformed to, by use of Eqs. (28),

$$\mathcal{E}(x_p, z+\Delta z) = \frac{1}{N} \sum_{m=-N/2+1}^{N/2} \mathcal{E}_m(z+\Delta z) \cdot \exp(j \frac{2\pi}{L} m \cdot x_p) \tag{29}$$

where $\quad \mathcal{E}_m(z+\Delta z) = \mathcal{E}_m(z) \cdot \exp \left[\frac{j\Delta z}{2k_s} (\frac{2\pi}{L} m)^2 \right]$

Eq. (29) is the inverse Fourier transform of $\mathcal{E}_m(z+\Delta z)$ in a homogeneous medium.

We now return back to the general case of in-

homogeneous media. With reference to Eq.(26) and (29), a general equation which relates $\mathcal{E}(x, z+\Delta z)$ and $\mathcal{E}(x, z)$ in any shaped waveguide structures becomes

$$\mathcal{E}(x_p, z+\Delta z) = \frac{1}{N} \sum_{m=-N/2+1}^{N/2} \mathcal{E}_m(z+\Delta z) \cdot \exp(j\frac{2\pi}{L} m \cdot x_p)$$
$$\cdot \exp\left[\frac{k_s \Delta z}{j2}\left(\frac{n^2(x, z+\Delta z/2)}{n_s^2}-1\right)\right] \tag{30}$$

where $\mathcal{E}_m(z+\Delta z) = \mathcal{E}_m(z) \cdot \exp\left[\frac{j\Delta z}{2k_s}\left(\frac{2\pi}{L}m\right)^2\right]$

$$\mathcal{E}_m(z) = \sum_{p=-N/2+1}^{N/2} \mathcal{E}(x_p, z) \cdot \exp(-j\frac{2\pi}{N} p \cdot m)$$

Once the index distribution of an arbitrary guiding structure is given, the effective index distribution $N(x,z)$ can be easily obtained by the procedure of Eq.(15) and (18). This earned $N(x,z)$ replaces $n(x,z)$ of Eq.(30) to perform the BPM.

B. BPM Simulation

As mentioned in Eq.(7) and (8), the substrate index including the channel region index will increase or decrease by δn when the electric field is applied. For an electric field applied, n_s of Eq.(12) becomes the function of position. $n_s(x)$ is modeled as the following

$$n_s(x) =$$

$$\left[\begin{array}{ll} n_s + \delta n & x \geq c_1 - w_1/2 \\[2ex] n_s + \dfrac{2\delta n}{[(c_1-w_1/2)-(c_2+w_2/2)]}[x-(c_1-w_1/2)]+\delta n \\[1ex] \qquad\qquad c_2 + w_2/2 \leq x \leq c_1 - w_1/2 \\[2ex] n_s - \delta n & x \leq c_2 + w_2/2 \end{array}\right. \tag{31}$$

In performing the BPM, the effective index $N(x)$ at an arbitrary z plane should be readily available. In fact, $N(x)$ is readily obtained by the procedure of Eq.(15) and (18).

However, the procedure for obtaining $N(x)$ needs to be slightly modified when the electric field is applied. Due to the change of n_s and n_t by δn,

V_y of Eq.(17) varies. Typical value of δn for Ti : $LiNbO_3$ is less than $10^{-4}/10V$. As the variation of V_y is almost negligible, V_y is assumed to remain unchanged. Consequently, b remains unchanged. When we consider δn variation of n_s in Eq.(12), it will be noticed that $N(x)$ also changes by δn in the channel regions. In more detail,

$$N(x) \Rightarrow N(x) + [n_s(x) - n_s] \tag{32}$$

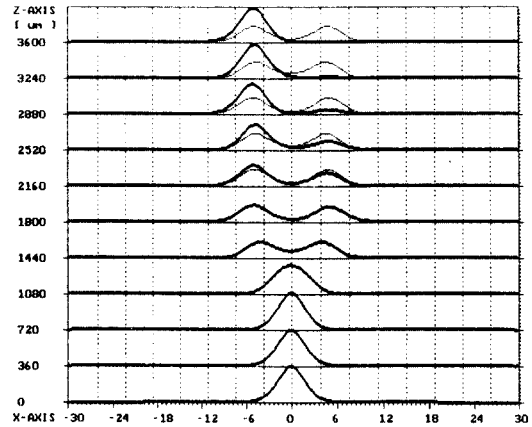Note that Eq.(32) is acceptable under the condition of weakly-guiding.

Fig. 2. BPM in Y-branch DC optical switch. Parallel arms start at $z = 1550\ \mu m$ $V_{sw} = 0$ V : thin curve, $V_{sw} = 13$ V : thick curve

In Fig.2, we illustrate how the beam mode changes while propagating along the z-axis when the electric field is not applied. The coupling length l_y is calculated to be around $2050\ \mu m$ while the normal mode theory estimates $2187\ \mu m$. For 13.0 V of applied voltage, switchning phenomenon is also illustrated in Fig.2. The extinction ratio, $10\log(P_{max}/P_{min})$, is as much as 17.3 dB.

IV. Experiment

Devices are built on z-cut $LiNbO_3$ substrate. Ti strip dimensions of the Y-branch DC prior to the
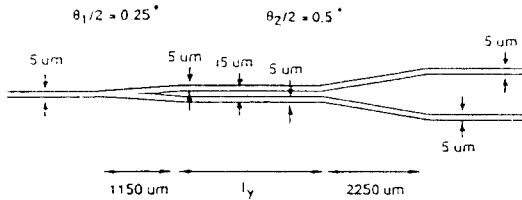
1113

diffusion is drawn in Fig.3.

Fig. 3. Detailed measure of the Y-branch directional coupler

As mentioned earlier, the Y-branch DC are fabricated by diffusing a 700 Å thick Ti film at 1025 ℃ for 6 hours in a wet oxygen atmosphere. The waveguides of the above fabrication parameters are theoretically and experimentally confirmed to support the single TM mode at $\lambda = 1.3$ μm.

1500 Å thick SiO_2 films are deposited in order to avoid the large insertion loss due to the metallic electrodes. RF sputtering technique is used for the depositing SiO_2 buffer layer. The deposited SiO_2 buffer layer is annealed at 600 ℃ for 4 hours in an oxygen atmosphere to eliminate the possibility of current leakage in the low-frequency (including dc) operation [7].
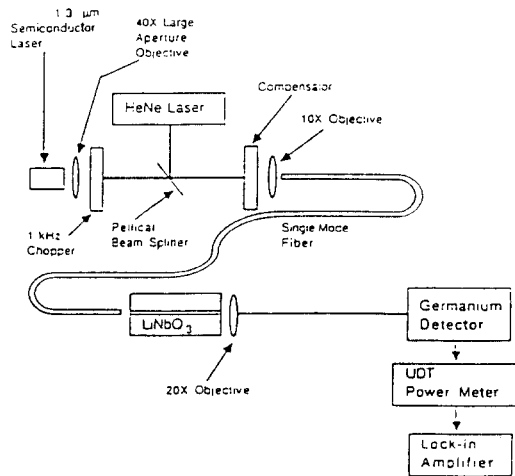

Fig. 4. A block diagram for the optical switching measurement

Al electrodes of semi-infinite coplanar strip structure are then situated on top of the waveguides in the coupler section. Inner edges of the Al electrodes are aligned with the inner edges of Ti prior to the diffusion to maximize the overlap integral between the optical field and the modulating electric field [4].

A block diagram for the optical dc switching measurement is illustrated in the Fig.4.

It is experimentally confirmed that l_y is 2.78 ㎜ at $\lambda = 1.3$ μm. Two devices of $L = l_y$ and $L = 0.75$ l_y are tested. No dc current leakage through the SiO_2 buffer layer is detected in both devices. For the devices of $L = l_y$, V_{sw} is as much as 12 V. Experimental results of optical power outputs are plotted with respect to $\Delta\beta L/\pi$ in Fig.5 and compared with the coupled mode theory's estimation.
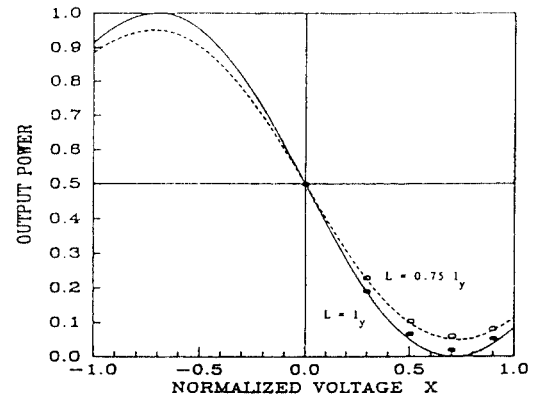

Fig. 5. Calculated(lines) and measured(dots) power output RR*. Solid line : $L = l_y$, dashed line : $L = 0.75$ l_y

The theoretical calculations and the experimentally measured values of l_y and V_{sw} are illustrated in the Table I.

Table I. Comparison of the theories' estimations and the experimental results

	l_y (μm)	V_{sw} (V)
Mode theory	2,187	11.45
BPM	2,050	13.0
Experiment	2,780	12.0

Ⅴ. Discussion

Several analysis approaches including the mc dal analyses and the BPM are made use of to design the Y-branch DC optical switches/modulators. The experiment is performed and compared with the theoretical results.

Two devices with different coupling lengths are fabricated and tested at the wave length $\lambda = 1.3 \ \mu m$. The dc switching operation with respect to the applied voltage $(\Delta\beta L/\pi)$ are in good agreement with the mode theories' expectation. However, there is a comparatively big discrepancy between the experimental l_y and the theoretical l_y. This may be attributed to some to lerances occurred in the process of the device's fabrication. On the other hand, the measured V_{sw} shows similar result as the estimated V_{sw}.

For a same structure of coupling section, the coupling length of the Y-branch DC is shorter than that of the uniform DC by the factor of $1/\sqrt{2}$ While maintaining lower switching voltage and the same extinction ratio. This reduction of the coupling length contributes to the higher-speed optical switching/modulation when we employ the traveling-wave electrode. In the future, many efforts need to be made for finding the optimum traveling-wave electrode design parameters to achieve the M/W impedance matching and the optical & M/W velocity matching.

References

1. S. Thaniyavarn, "Modified 1×2 directional coupler waveguide modulator," Electron. Lett., Vol. 22, No.18, p.941, 28 August 1986.

2. M. D. Feit and J. A. Fleck, Jr., "Computation of mode properties in optical fiber waveguides by a propagating beam method," Applied Optics, vol.19, No.7, p.1154, April 1980.

3. T. Tamir, Topics in Applied Physics : Integrated optics, 2nd Edition, Berlin : Springer-Verlag, p.71-p.73, 1979.

4. C.M. Kim and R.V. Ramaswamy, "Overlap integral factors in integrated optic modulators and switches," IEEE J. Lightwave Technol., Vol.7, No.7, p.1063, July 1989.

5. C.M. Kim and R.V. Ramaswamy, "Modeling of graded-index channel waveguide using nonuniform finite-difference method," IEEE J. Lightwave Technol., Vol.LT-7, No.10, p.1581, October 1989.

6. C.M. Kim and R.V. Ramaswamy, "WKB analysis of asymmetric directional couplers and its application to optical switches," IEEE J. Lightwave Technol., Vol.6, No.6, p.1109, June 1988.

7. G.L. Tangonan, D.L. Persechini, J.F. Lotspeich and M.K. Barnoski, "Electrooptic diffration modulation in Ti-diffused LiTaO₃," Appl. Optics, Vol.17, No.20, p.3259, 15 October 1978.
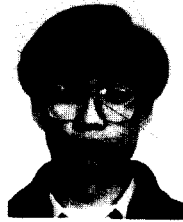
1115

金 昌 敏(Chang Min Kim) 正會員
1950년 4월 10일생
1975년 2월 : 서울대학교 전자공학
과 공학사
1982년 2월 : 서울대학교 전자공학
과 공학석사
1989년 8월 : Univ. of Florida 전자
공학과 공학박사
1983년~현재 : 서울시립대학교 전자공학과 부교수
● 주전공분야 : 집적광학
※주관심분야 : 전자파, 광파 및 양자전자.

韓 相 弼(Sang-Pil Han)   정회원
1964年 5月 9日生
1992년 2월 : 서울市立大學校 電子
工學科 卒業
1992년 3월~현재 : 서울市立大學
校 大學院 電子工學科
碩士課程 在學中
※主關心分野 : 光電子工學, 量子電
子工學

宋 洛 靈(Nag Un Song)   정회원
1975년 2월 : 서울대 전자과 졸업(BS)
1977년 2월 : 서울대학원 전자과 졸업(MS)
1986년 5월 : Univ. Texas, Austin(Ph.D)
1986년 8월~1989년 8월 : 금성반도체 책임연구원
1989년 9월~현재 : 홍대 전자과 조교수
※주관심분야 : 수치해석(FDM, FEM) 회로설계